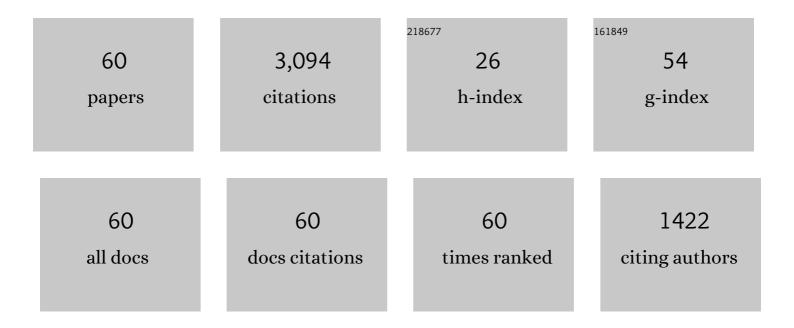
Zhongyu Cui

List of Publications by Year in descending order

Source: https://exaly.com/author-pdf/1364552/publications.pdf Version: 2024-02-01



#	Article	IF	CITATIONS
1	Roles of pH in the NH4+-induced corrosion of AZ31 magnesium alloy in chloride environment. Journal of Magnesium and Alloys, 2022, 10, 3167-3178.	11.9	8
2	Passivation Behavior of 2507 Super Duplex Stainless Steel in Hot Concentrated Seawater: Influence of Temperature and Seawater Concentration. Acta Metallurgica Sinica (English Letters), 2022, 35, 326-340.	2.9	16
3	Effect of extrusion on the microstructure and corrosion behavior of Mg-Zn-Mn-(0, 1.5)Sr alloys in Hank's solution. Corrosion Science, 2022, 195, 109975.	6.6	27
4	The influence of Nb addition on the passivity of CoCrNiNb multi-principal element alloys. Journal of Electroanalytical Chemistry, 2022, 908, 116107.	3.8	4
5	Effect of temperature and dissolved oxygen on the passivation behavior of Ti–6Al–3Nb–2Zr–1Mo alloy in artificial seawater. Journal of Materials Research and Technology, 2022, 17, 374-391.	5.8	24
6	Correlation between low-temperature anticorrosion performance and mechanical properties of composite coatings reinforced by modified Fe3O4. Progress in Organic Coatings, 2022, 165, 106737.	3.9	3
7	Understanding the passivation behavior and film chemistry of four corrosion-resistant alloys in the simulated flue gas condensates. Materials Today Communications, 2022, 31, 103567.	1.9	3
8	Corrosion behavior of CoCrNiMoBC coatings obtained by laser cladding: Synergistic effects of composition and microstructure. Journal of Alloys and Compounds, 2022, 911, 164984.	5.5	8
9	Corrosion evolution and stress corrosion cracking behavior of a low carbon bainite steel in the marine environments: Effect of the marine zones. Corrosion Science, 2022, 206, 110490.	6.6	42
10	Quantitative study of the corrosion evolution and stress corrosion cracking of high strength aluminum alloys in solution and thin electrolyte layer containing Cl Corrosion Science, 2021, 178, 109076.	6.6	105
11	Correlation between Microstructure and Hydrogen Degradation of 690 MPa Grade Marine Engineering Steel. Materials, 2021, 14, 851.	2.9	3
12	Passivation behavior and surface chemistry of 316 SS in the environment containing Clâ^' and NH4+. Journal of Electroanalytical Chemistry, 2021, 886, 115138.	3.8	10
13	Elucidating the passivation kinetics and surface film chemistry of 254SMO stainless steel for chimney construction in simulated desulfurized flue gas condensates. Construction and Building Materials, 2021, 285, 122905.	7.2	17
14	Recycling papermill waste lignin into recyclable and flowerlike composites for effective oil/water separation. Composites Part B: Engineering, 2021, 216, 108884.	12.0	20
15	Effect of NH4+ on the pitting corrosion behavior of 316 stainless steel in the chloride environment. Journal of Electroanalytical Chemistry, 2021, 894, 115368.	3.8	19
16	Hydrogen permeation and stress corrosion cracking of heat-affected zone of E690 steel under the combined effect of sulfur species and cathodic protection in artificial seawater. Construction and Building Materials, 2021, 296, 123721.	7.2	15
17	Anticorrosion behavior of organic offshore coating systems in UV, salt spray and low temperature alternation simulated Arctic offshore environment. Materials Today Communications, 2021, 28, 102545.	1.9	6
18	The anti-corrosion performance of the epoxy coating enhanced via 5-Amino-1,3,4-thiadiazole-2-thiol grafted graphene oxide at ambient and low temperatures. Progress in Organic Coatings, 2021, 159, 106441.	3.9	9

ZHONGYU CUI

#	Article	IF	CITATIONS
19	Passivation behavior of CoCrNiZr medium-entropy alloy in the sulfuric acid solutions. Journal of Electroanalytical Chemistry, 2021, 899, 115693.	3.8	6
20	Understanding the effect of fluoride on corrosion behavior of pure titanium in different acids. Corrosion Science, 2021, 192, 109812.	6.6	38
21	Influence of sulfide on the passivation behavior and surface chemistry of 2507 super duplex stainless steel in acidified artificial seawater. Applied Surface Science, 2020, 504, 144340.	6.1	29
22	Characterization of the passive properties of 254SMO stainless steel in simulated desulfurized flue gas condensates by electrochemical analysis, XPS and ToF-SIMS. Corrosion Science, 2020, 165, 108405.	6.6	66
23	Corrosion evolution and stress corrosion cracking of E690 steel for marine construction in artificial seawater under potentiostatic anodic polarization. Construction and Building Materials, 2020, 238, 117763.	7.2	63
24	Siloxane-epoxy composite coatings for enhanced resistance to large temperature variations. Progress in Organic Coatings, 2020, 139, 105457.	3.9	11
25	Anticorrosion behavior of superhydrophobic particles reinforced epoxy coatings for long-time in the high salinity liquid. Progress in Organic Coatings, 2020, 147, 105867.	3.9	4
26	Influence of Rare Earth Element (Y) on Microstructure and Corrosion Behavior of Hot Extrusion AZ91 Magnesium Alloy. Materials, 2020, 13, 3651.	2.9	13
27	Dissolution kinetics of the sulfide-oxide complex inclusion and resulting localized corrosion mechanism of X70 steel in deaerated acidic environment. Corrosion Science, 2020, 174, 108815.	6.6	50
28	The effect of crack tip environment on crack growth behaviour of a low alloy steel at cathodic potentials in artificial seawater. Journal of Materials Science and Technology, 2020, 54, 119-131.	10.7	25
29	Pitting behavior of SLM 316L stainless steel exposed to chloride environments with different aggressiveness: Pitting mechanism induced by gas pores. Corrosion Science, 2020, 167, 108520.	6.6	129
30	Mechanistic study of ammonium-induced corrosion of AZ31 magnesium alloy in sulfate solution. Journal of Materials Science and Technology, 2020, 54, 1-13.	10.7	20
31	Combined effect of cathodic potential and sulfur species on calcareous deposition, hydrogen permeation, and hydrogen embrittlement of a low carbon bainite steel in artificial seawater. Corrosion Science, 2019, 158, 108089.	6.6	98
32	Electrochemical and XPS analytical investigation of the accelerative effect of bicarbonate/carbonate ions on AISI 304 in alkaline environment. Applied Surface Science, 2019, 492, 792-807.	6.1	55
33	Fabrication of durable and roughness-regeneration superhydrophobic composite materials by hot pressing. Composites Part B: Engineering, 2019, 179, 107431.	12.0	25
34	Effect of alloyed Sr on the microstructure and corrosion behavior of biodegradable Mg-Zn-Mn alloy in Hanks' solution. Corrosion Science, 2019, 157, 420-437.	6.6	109
35	Influence of different heat-affected zone microstructures on the stress corrosion behavior and mechanism of high-strength low-alloy steel in a sulfurated marine atmosphere. Materials Science & Engineering A: Structural Materials: Properties, Microstructure and Processing, 2019, 759, 124-141.	5.6	77
36	Facile fabrication of hydrophobic polysiloxane coatings for protection of AZ31 magnesium alloy. Journal of Materials Science, 2019, 54, 9759-9774.	3.7	10

ZHONGYU CUI

#	Article	IF	CITATIONS
37	Passivation behavior and surface chemistry of 2507 super duplex stainless steel in artificial seawater: Influence of dissolved oxygen and pH. Corrosion Science, 2019, 150, 218-234.	6.6	212
38	The effect of sub-grain structure on intergranular corrosion of 316L stainless steel fabricated via selective laser melting. Materials Letters, 2019, 243, 157-160.	2.6	57
39	Influence of inclusions on initiation of pitting corrosion and stress corrosion cracking of X70 steel in near-neutral pH environment. Corrosion Science, 2019, 147, 108-127.	6.6	158
40	Characterization of the Outer Layer Nanostructure in the Electrochemical Response of Stainless Steel in Aqueous Sodium Hydroxide. Analytical Letters, 2018, 51, 1384-1399.	1.8	8
41	A comparative study of primary and secondary passive films formed on AM355 stainless steel in 0.1 M NaOH. Applied Surface Science, 2018, 427, 763-773.	6.1	96
42	Electrochemical corrosion, hydrogen permeation and stress corrosion cracking behavior of E690 steel in thiosulfate-containing artificial seawater. Corrosion Science, 2018, 144, 145-162.	6.6	129
43	Simple spray deposition of a hot water-repellent and oil-water separating superhydrophobic organic-inorganic hybrid coatings via methylsiloxane modification of hydrophilic nano-alumina. Progress in Organic Coatings, 2018, 125, 15-22.	3.9	20
44	Corrosion behavior of AZ31 magnesium alloy in the chloride solution containing ammonium nitrate. Electrochimica Acta, 2018, 278, 421-437.	5.2	78
45	Combined Effect of Alternating Current Interference and Cathodic Protection on Pitting Corrosion and Stress Corrosion Cracking Behavior of X70 Pipeline Steel in Near-Neutral pH Environment. Materials, 2018, 11, 465.	2.9	24
46	Electrochemical Behavior and Surface Characteristics of Pure Titanium during Corrosion in Simulated Desulfurized Flue Gas Condensates. Journal of the Electrochemical Society, 2018, 165, C542-C561.	2.9	56
47	Influence of temperature on the electrochemical and passivation behavior of 2507 super duplex stainless steel in simulated desulfurized flue gas condensates. Corrosion Science, 2017, 118, 31-48.	6.6	257
48	Passivation Behavior and Surface Chemistry of 2507 Super Duplex Stainless Steel in Acidified Artificial Seawater Containing Thiosulfate. Journal of the Electrochemical Society, 2017, 164, C856-C868.	2.9	51
49	Mechanistic studies of atmospheric corrosion behavior of Al and Al-based alloys in a tropical marine environment. Journal Wuhan University of Technology, Materials Science Edition, 2017, 32, 633-639.	1.0	4
50	Effect of plastic deformation on the electrochemical and stress corrosion cracking behavior of X70 steel in near-neutral pH environment. Materials Science & Engineering A: Structural Materials: Properties, Microstructure and Processing, 2016, 677, 259-273.	5.6	116
51	Anodic Dissolution Behavior of the Crack Tip of X70 Pipeline Steel in Near-Neutral pH Environment. Journal of Materials Engineering and Performance, 2016, 25, 5468-5476.	2.5	6
52	Comparative study of the SCC behavior of E690 steel and simulated HAZ microstructures in a SO2-polluted marine atmosphere. Materials Science & Engineering A: Structural Materials: Properties, Microstructure and Processing, 2016, 650, 93-101.	5.6	50
53	Effect of pH Value on the Crack Growth Behavior of X70 Pipeline Steel in the Dilute Bicarbonate Solutions. Materials Transactions, 2015, 56, 777-780.	1.2	6
54	Atmospheric Corrosion Behavior of 2A12 Aluminum Alloy in a Tropical Marine Environment. Advances in Materials Science and Engineering, 2015, 2015, 1-17.	1.8	13

ZHONGYU CUI

#	Article	IF	CITATIONS
55	Corrosion Behavior of Field-Exposed Zinc in a Tropical Marine Atmosphere. Corrosion, 2014, 70, 731-748.	1.1	43
56	Atmospheric corrosion of field-exposed AZ31 magnesium in a tropical marine environment. Corrosion Science, 2013, 76, 243-256.	6.6	137
57	Corrosion of hot extrusion AZ91 magnesium alloy: I-relation between the microstructure and corrosion behavior. Corrosion Science, 2011, 53, 1960-1968.	6.6	226
58	Corrosion of hot extrusion AZ91 magnesium alloy. Part II: Effect of rare earth element neodymium (Nd) on the corrosion behavior of extruded alloy. Corrosion Science, 2011, 53, 2934-2942.	6.6	170
59	Corrosion Evolution of High-Strength Aluminum Alloys in the Simulated Service Environment of Amphibious Aircraft in the Presence of Chloride and Bisulfite. Acta Metallurgica Sinica (English) Tj ETQq1 1 0.784	3 1249rg BT	/Overlock 10
60	The crevice corrosion behavior of N80 carbon steel in acidic NaCl solution: The effect of O 2. Materials and Corrosion - Werkstoffe Und Korrosion, 0, , .	1.5	3